Semiconductor Physics, Quantum Electronics & Optoelectronics, 2024. V. 27, No 4. P. 418-426.

Semiconductor physics

The effect of substrate bias voltage on the properties of Al-doped ZnO films deposited by magnetron sputtering

A.I. Ievtushenko[1*], V.A. Karpyna[1], O.F. Kolomys[2], S.V. Mamykin[2], P.M. Lytvyn[2], O.I. Bykov[1], A.A. Korchovyi[2], S.P. Starik[3], V.V. Bilorusets[3], V.I. Popenko[2], V.V. Strelchuk[2], V.A. Baturin[4], O.Y. Karpenko[4]

[1]*I. Frantsevych Institute for Problems of Materials Science, NASU, Kyiv, Ukraine*
[2]*V. Lashkaryov Institute of Semiconductor Physics, NASU, Kyiv, Ukraine*
[3]*V. Bakul Institute for Superhard Materials, NASU, Kyiv, Ukraine*
[4]*Institute of Applied Physics, NASU, Sumy, Ukraine*
[*]*Corresponding author e-mail: a.ievtushenko@ipms.kyiv.ua*

Abstract. Our work aims to investigate the influence of substrate bias voltage on the structure, optical, and electrical properties of ZnO:Al thin films deposited on Si (100) and glass substrates by radio frequency magnetron sputtering. We have applied the layer-by-layer growth method in magnetron sputtering. X-ray diffraction, atomic force microscopy, Raman scattering, photoluminescence, Fourier transform infrared spectrometry, multi-angle spectral ellipsometry, optical transmission, and electrical measurements were used to characterize samples. It was found that the negative bias voltage applied to the substrate holder during film growth caused an increase in the conductivity of ZnO:Al films four times compared with ZnO:Al films grown without external bias voltage. The concentration of Al donor impurity was increased in ZnO:Al films with increasing the negative bias voltage applied to the substrate.

Keywords: ZnO:Al films, magnetron sputtering, substrate bias voltage, transmittance, XRD, electrical conductivity.

https://doi.org/10.15407/spqeo27.04.418
PACS 68.55.Ln, 77.55.hf, 79.60.-i

Manuscript received 05.08.24; revised version received 26.09.24; accepted for publication 13.11.24; published online 06.12.24.

1. Introduction

Transparent conductive oxides (TCO) are important materials for many industrial equipment and home appliances. Indium tin oxide (ITO) is a well-known TCO, which was successfully industrialized due to its electrical, optical, and technological advantages. Nowadays, there is a trend toward developing a cost-effective indium-free TCO as world reserves of indium are limited. ZnO is a wide band gap semiconductor material that is prospective not only for indium-free TCO development but also for the development of light emitting devices, ultraviolet detectors, gas sensors, and photocatalysts [1–5] with increased resistance to electron irradiation [6]. ZnO is a good dielectric material but doping with aluminium, gallium or indium transforms ZnO into a very conductive and transparent making it the best choice to replace ITO. We believe that the development of a highly efficient deposition technology for Al-doped ZnO TCO films will have a commercial future.

Magnetron sputtering is the most widely used method for TCO film deposition due to high deposition rates, low temperature of deposition, good film uniformity, adhesion, and easy control over technology parameters [7]. There are many papers aimed at improving the ZnO:Al films properties by changing the oxygen pressure, magnetron power, and substrate temperature [8–10]. Obviously, the influence of bias voltages applied to a substrate (substrate bias voltage) on the structure, optical, and electrical properties of Al-doped ZnO films was not studied very well. The effect of negative substrate bias voltage on the strain properties of ZnO films was studied in [11]. Stoichiometry control of ZnO by applying substrate bias voltage was studied in [12, 13]. The effect of positive substrate bias voltage on Al-doped ZnO TCO films was studied in [14]. The authors state that a positive bias voltage applied to the substrate during sputtering caused the improvement of the electrical properties of the film by accelerating the plasma electrons that bombarded the growing films. This bombardment provided an additional energy to the growing ZnO:Al film, significantly variating the film structure and electrical properties.

Therefore, our work aims to investigate the influence of the substrate bias voltage on the structure, optical and electrical properties of ZnO:Al thin films deposited on Si (100), Si (111), and glass substrates by using the layer-by-layer growth method at magnetron sputtering.

2. Experimental

ZnO:Al thin films were deposited on Si (100) and glass substrates using the layer-by-layer growth method [15, 16] at radio frequency magnetron sputtering. The metallic Zn-Al composite target was sputtered in the argon-oxygen atmosphere under the following deposition parameters: the partial pressures of oxygen and argon were close to 0.05 and 1 Pa, respectively. Magnetron power was 250 W, and substrate temperature T_s was 300 °C. The substrate bias voltage (V_{sb}) was changed as follows: 0, +2, –15, and –30 V.

The crystal structure was investigated by X-ray diffraction (XRD) using a DRON-4 diffractometer with Cu-Kα radiation (λ = 0.1542 nm). Elemental analysis was carried out by ZEISS EVO 50 XVP SEM (Zeiss, Germany) setup by using energy dispersive X-ray (EDX) equipment with Ultim Max 100 analyzer (Oxford Instruments, England). Raman measurements were carried out in a quasi-backscattering geometry using a Horiba Jobin-Yvon T64000 triple spectrometer with an integrated micro-Raman setup – Olympus BX-41 microscope equipped with a Peltier-cooled CCD detector. The experiments were carried out at room temperature by using the 488 nm line of an Ar/Kr laser. Photoluminescence (PL) spectra of samples were recorded with the help of He-Cd laser excitation at room temperature. The FTIR reflectance measurements have been performed using a vacuum Fourier transform spectrometer Bruker Vertex 70V at room temperature. The sample transmission spectra were recorded on a computerized monochromator LOMO12 equipped with a Hamamatsu Si photodiode. The spectral dependences of optical constants and film thickness were measured by multi-angle spectral ellipsometry (MSE) on a setup SE-2000 from SEMILAB. The spectral analysis was performed using the software SEA (WinElli 3) 1.5.44. The surface morphology of deposited films was studied using an atomic force microscope (AFM) (Quadrexed NanoScope IIIa Dimension 3000, Digital Instruments/Bruker, USA) in the tapping mode (periodic contact of silicon probe with a nominal radius 10 nm). The root-mean-square (RMS) values of film flatness and the average grain size are ascertained from the most typical fragment of the film surface with an area of 5×5 μm. The resistivity of Al-doped ZnO thin films was determined by the Van der Pauw method in the dark by the Keithley-236 Source Measure Unit.

3. Results and discussion

XRD patterns of ZnO:Al films deposited at various V_{sb} are shown in Fig. 1. We can see that all deposited samples are single-phase and highly textured ZnO polycrystalline films with wurtzite crystal structures that are confirmed by intensive reflections from (002) planes. The observation of only (002) and (004) XRD peaks on 2θ spectra implies that films are grown with their *c*-axis oriented perpendicular to the substrate. An interesting phenomenon has been observed for the (002) peak of ZnO:Al sample grown at V_{sb} = –15 V: the XRD (002) peak is split and consists of two separate XRD peaks, which are reflections of the same (002) plane, but from two differently strained regions of the material (see Fig. 1, insertion). In this case, Gauss fitting gives us two peak positions at 33.75 and 34.16 degrees with a FWHM (full width at half maximum) value of 0.44 degrees for the first peak and 1.1 degrees for the second one. ZnO crystal lattice parameters and grain sizes ascertained from XRD measurements are summarized in Table 1. One can see that ZnO:Al films grown with V_{sb} = 15 V demonstrate the distinct grain sizes 25 and 8 nm with different stresses of 0.02 and 0.008, respectively. The

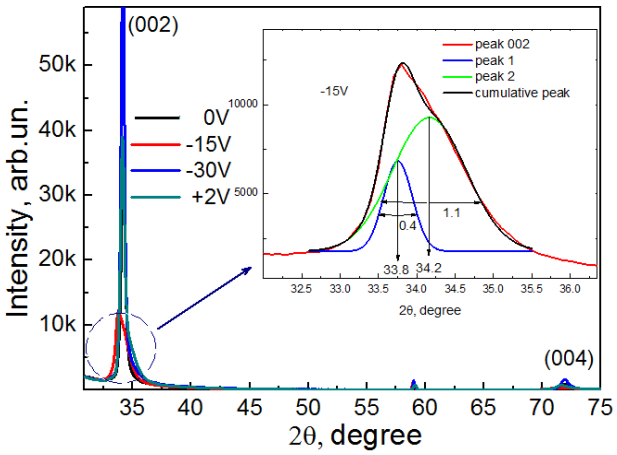

Fig. 1. XRD patterns of ZnO:Al films deposited on Si substrates by magnetron sputtering at different substrate bias voltage V_{sb}. The insertion presents an enlarged XRD pattern of ZnO:Al films deposited at V_{sb} = –15 V with decomposition on elementary Gaussians. For interpretation of the colors in the figure(s), the reader is referred to the web version of this article.

Table 1. ZnO crystal lattice parameters, strain, and grain sizes ascertained from XRD measurements.

Substrate bias voltage, *V*	(002) peak position, degree	(002) peak FWHM, degree	Interplanar spacing *d*, nm	Lattice constant *c*, nm	Strain ε,	Grain size, nm
0	34.19	0.42	0.2623	0.5245	0.007	20
+2	34.15	0.43	0.2625	0.5251	0.009	19
–15	33.75 34.16	0.44 1.1	0.2656 0.2625	0.5311 0.5249	0.020 0.008	25 8
–30	34.16	0.34	0.2625	0.5249	0.008	25

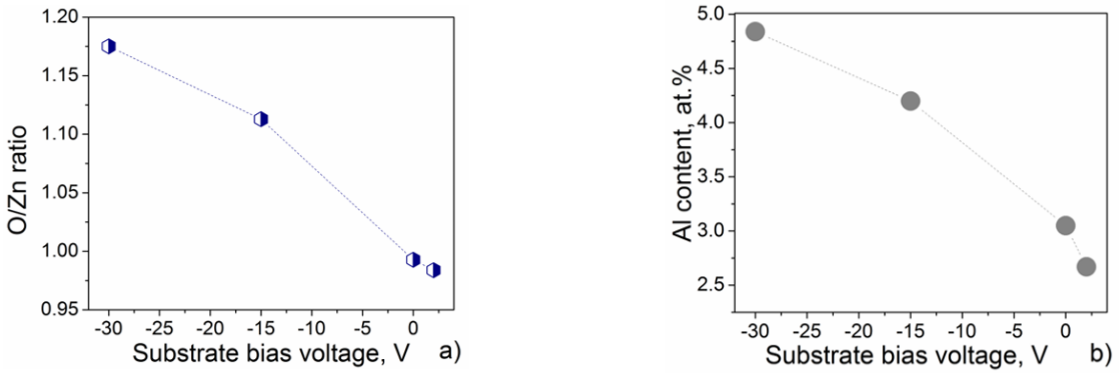

Fig. 2. The O/Zn ratio (a) and Al concentration (b) of ZnO:Al films deposited on Si substrates by magnetron sputtering at different substrate bias voltage V_{sb}.

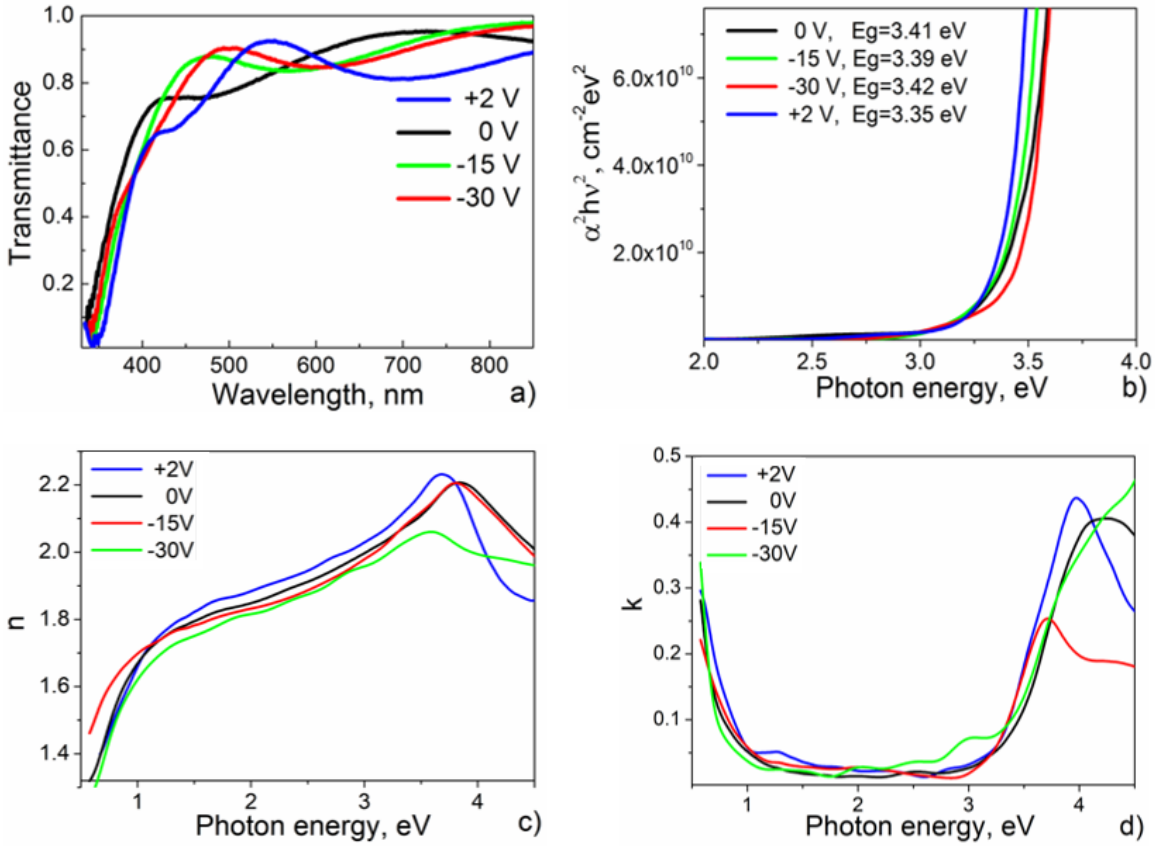

Fig. 3. The spectra of optical transmittance (a), optical band gap (b), refractive index n (c), and extinction coefficient k (d) of ZnO:Al films deposited on glass (a, b) and Si (c, d) substrates by magnetron sputtering at different substrate bias voltage V_{sb}.

lowest FWHM value was observed for ZnO:Al films grown with the highest negative V_{sb} = 30 V. This film demonstrates the best crystalline quality.

The elemental composition of ZnO:Al films studied by EDX spectroscopy is shown in Fig. 2. Increasing negative voltage on the substrate causes an increase in the O/Zn ratio from 0.98 to 1.18, indicating an increase in the oxygen content of ZnO:Al films. Thus, the concentration of oxygen vacancies should be decreased. Simultaneously, Al concentration increases with negative bias voltage improving the incorporation of Al donor impurity into ZnO lattice.

The optical transmittance spectra of ZnO:Al films grown at various V_{sb} are shown in Fig. 3. Fig. 3b demonstrates the same spectra in coordinates $\alpha^2 h\nu^2 = f(h\nu)$ for optical band gap (E_g) calculation. As one can see, the optical band gap is within the range 3.35…3.42 eV. The lowest value E_g was observed for ZnO:Al films grown at

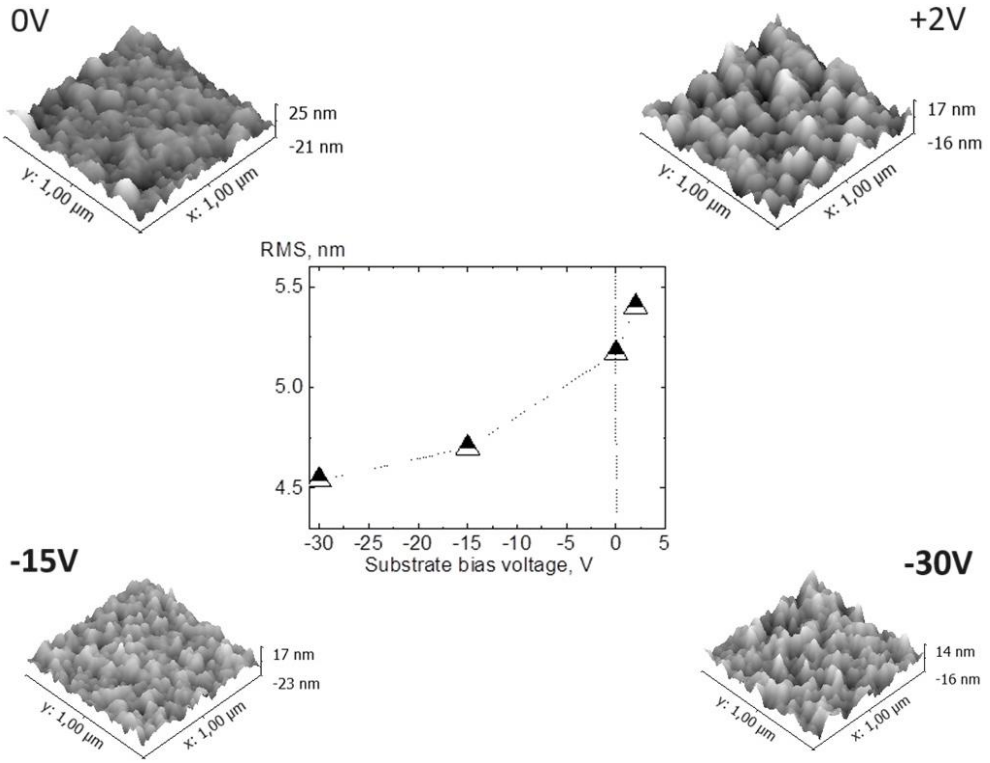

Fig. 4. The AFM images of ZnO:Al films with the surface RMS values (figure in the insertion) deposited on Si substrates by magnetron sputtering at different substrate bias voltage V_{sb}.

positive V_{sb}. For ZnO:Al films grown at negative V_{sb} the value of E_g is within 3.39…3.42 eV. The same behavior of the band gap with applied V_{sb} was ascertained using the optical spectra of refractive index (Fig. 3c) and extinction coefficient (Fig. 3d) calculated using the results of multi-angle spectral ellipsometry. The sharp decrease in n and increase in k within the range 0.5…1.0 eV are probably caused by a strong influence of free carriers on our optical spectra (Figs 3c, 3d). The intensive peak close to 3.5 eV corresponds to exciton, confirming that the deposited films are highly conductive and have good quality [17].

The results of MSE allow us to calculate the values of film thickness (d), roughness, mobility, and concentration of electrons, as well as estimate the optical resistivity of the films. To calculate the above-mentioned parameters, we used the calculation method in the Tanguy and Drude models, described in detail in our work [17]. The calculated parameters for the ZnO:Al thin films deposited on Si substrates according to these models are given in Table 2. Thus, we found out that the thickness of the films varied within 204…296 nm, roughness – within 23… 63 nm, electron mobility – within 11…29 $cm^2/(V{\cdot}s)$, and electron concentration – within 1.1… 1.7×10^{20} cm^{-3}, respectively. Our results show that as the O/Zn ratio increases with the applied negative V_{sb}, the concentration of electrons decreases while their mobility increases significantly, so the resulting resistivity decreases. The lowest value of film resistivity 1.6 mOhm·cm was observed at V_{sb} = –30 V.

AFM images of the surface morphology of ZnO:Al films grown at different V_{sb} are shown in Fig. 4. One can see that the grain sizes of ZnO:Al samples grown at 0 V and +2 V are larger than the ones grown at negative V_{sb}. The calculated RMS values presented in the insertion of Fig. 4 also confirm that the films grown at negative V_{sb} have smoother surfaces than other samples. The RMS values are decreased with the negative voltage applied to the substrate due to the deposition rate slowdown.

Table 2. The characteristics of ZnO:Al thin films grown on Si substrate, ascertained from the Tanguy and Drude models.

V_{sb}, V	Thickness d, nm	Roughness, nm	n-type dopant concentration, cm^{-3}	Mobility, $cm^2/(V{\cdot}s)$	Resistivity, mOhm·cm
+2	296	30	$1.7 \pm 0.02{\cdot}10^{20}$	17.7 ± 0.6	2.1 ± 0.1
0	204	23	$1.4 \pm 0.01{\cdot}10^{20}$	22 ± 1	2.1 ± 0.1
–15	256	37	$1.1 \pm 0.01{\cdot}10^{20}$	11.1 ± 0.5	5.0± 0.2
–30	267	63	$1.3 \pm 0.01{\cdot}10^{20}$	28.8 ± 0.9	1.6 ± 0.1

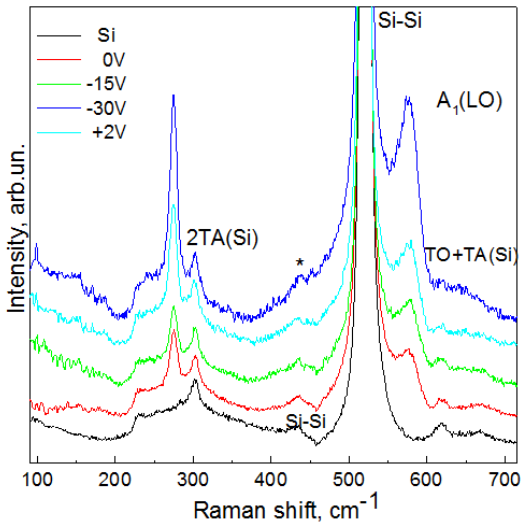

Fig. 5. The Raman spectra of ZnO:Al films deposited on Si substrates by magnetron sputtering at different substrate bias voltage V_{sb}.

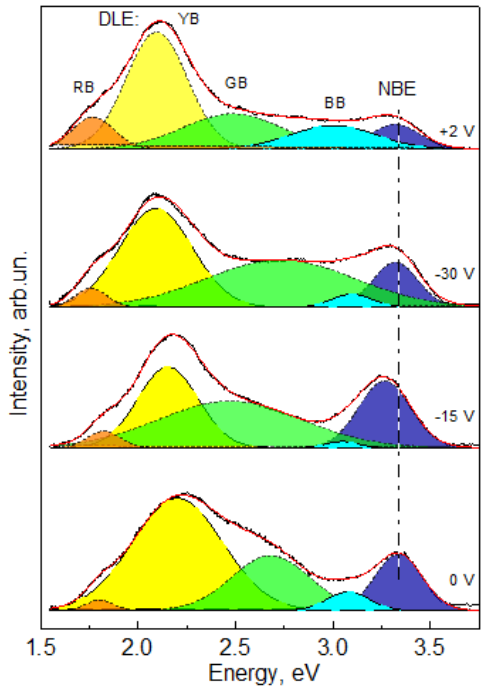

Fig. 6. The photoluminescence spectra of ZnO:Al films deposited on Si substrates by magnetron sputtering at different substrate bias voltage V_{sb}. The energy of excitation photons E_{exc} = 3.81 eV. T = 300 K.

Fig. 5 shows the 300 K Raman spectra of Si substrate (spectrum *1*) and ZnO:Al films (spectra *2–5*) acoustic 2TA, local Si-Si, and combination TA+TO the Raman spectrum consists of the vibrational bands at 302, 435, 520, and 619 cm^{-1} attributed to the transverse deposited at different V_{sb}. For the Si substrate, phonon modes, respectively. The Raman bands close to 276 and 576 cm^{-1}, related to crystal-lattice perfection, were observed for all ZnO:Al films. The weak band observed at 576 cm^{-1} is attributed to the A_1 (LO) mode of ZnO. The Raman scattering cross-section of the LO phonons is determined by both optical deformation potential and Fröhlich electron-phonon interaction [18]. However, the break-down of translational symmetry due to structural disorder caused by random incorporation of the dopant will lead to the fluctuations of alloy scattering potential. The intensity of the mentioned Raman band A_1 (LO) increases with increasing V_{sb} due to the increase in the concentration of zinc and oxygen interstitial (Zn_i, O_i) [19] and oxygen vacancy (V_O) [20] in the ZnO lattice of ZnO:Al films.

The origin of the next prominent Raman band at 276 cm^{-1} is still debated and controversial. In the work [21] Kaschner *et al*. observed this mode for the nitrogen-doped ZnO films and showed that its intensity correlates linearly with the nitrogen concentration. Also, this mode at 276 cm^{-1} and additional peaks close to 639, 716, and 858 cm^{-1} were partly observed for undoped ZnO films and nanostructures and for doped by different elements [22, 23]. Artus *et al.* [24] showed that these additional modes can be related to local impurity mode due to the incorporation of nitrogen atoms into the anion ZnO sublattice. In the work [25], Souissi *et al*. showed that the Raman band at 275 cm^{-1} can be assigned as B_1^{low} corresponding to the antiparallel shifts of only Zn atoms along the *c*-axis (*z*-axis). In any case, the presence of this phonon mode is induced by the crystal lattice imperfection due to intrinsic defects and impurities.

Fig. 6 shows the PL spectra of ZnO:Al films recorded at 300 K with the excitation at 3.81 eV. One can see, the films exhibit a wide band within the ultraviolet (UV) range and defect-related bands within the visible range. The band at 3.35 eV in the spectrum of ZnO:Al films grown at 0 V, related to the near band-edge (NBE) emission, indicates a decrease in the band gap compared to bulk ZnO (3.37 eV at room temperature). The large FWHM of the NBE emission band is caused by the presence of several recombination centers, different impurities, grain boundaries, and defects.

With increasing the substrate bias voltage, the UV emission band of as-grown ZnO:Al film demonstrates a nonmonotonic shift towards low energy and intensity enhancement, which can be explained by the increase in the grain size. The band gap of the small nanoparticles is slightly larger than that of the bulk materials. The visible deep-level emission (DLE) in the spectra of ZnO:Al films is the superposition of the red-orange band (ROB) at 2.08 eV, yellow band (YB) at 2.25 eV, and green emissions band (GB) at 2.55 eV (please see the results of deconvolution of DLE band in Fig. 6). These bands are usually associated with structural defects, particularly the oxygen interstitials, oxygen and zinc vacancy, and the surface states [26, 27]. With increasing the substrate bias voltage, the redistribution of the intensity of the red-orange emission band at 2.08 eV and yellow band at 2.25 eV is observed, which can be caused by the variation in surface states.

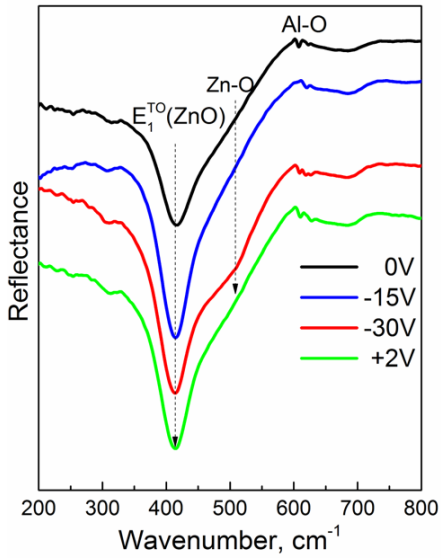

Fig. 7. The FTIR spectra of ZnO:Al films deposited on Si substrates by magnetron sputtering at different substrate bias voltage V_{sb}.

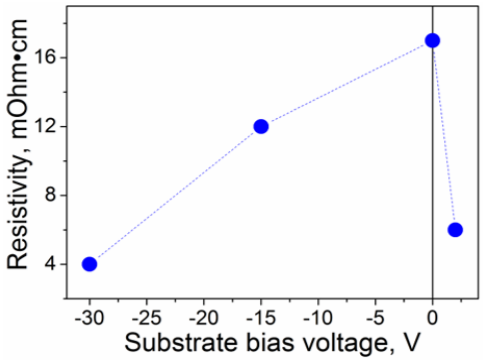

Fig. 8. The specific resistivity of ZnO:Al films deposited on glass substrates by magnetron sputtering at different substrate bias voltage V_{sb}.

The FTIR transmission spectra of ZnO:Al films deposited at different V_{sb} within the range 200…800 cm^{-1} are shown in Fig. 7. The main band at 414 cm^{-1} is attributed to the A_1(TO) phonon mode, and the high-frequency shoulder at 470 cm^{-1} is attributed to Zn-O stretching vibrations. The Zn-O absorption band is intensive for ZnO:Al films deposited at –30 V and +2 V substrate voltage, indicating the higher crystal quality of these films compared to ZnO:Al films grown at 0 V and small negative V_{sb} values. The weak absorption peak of the Al-O bond vibrations was observed at ~609 cm^{-1}.

Fig. 8 demonstrates the specific resistivity of ZnO:Al films measured by Van der Pauw method *vs* the applied substrate bias voltage V_{sb}. At zero V_{sb} the specific resistivity is equal to 17 mOhm·cm. Both negative and positive V_{sb} lead to a decrease in the specific resistivity of ZnO:Al films. The lowest value of the specific resistivity 4 mOhm·cm was achieved at –30 V_{sb}. Thus, by applying a negative bias voltage to the substrate, one can improve the conductivity of ZnO:Al films. This improvement is caused by the more effective Al^{3+} ions embedding into the ZnO lattice as a donor impurity.

4. Conclusions

The ZnO:Al thin films were deposited on Si (100) and glass substrates using the layer-by-layer growth method in radio frequency magnetron sputtering of metallic Zn-Al composite target. The substrate bias voltage was varied as 0, +2, –15, and –30 V at fixed other technological parameters.

The XRD results showed that the lowest FWHM value was observed for ZnO:Al films grown with the highest negative voltage bias –30 V. This film demonstrates the best crystalline quality, having grain sizes close to 25 nm. The increase in the negative voltage applied to the substrate leads to an increase in the O/Zn ratio from 0.98 to 1.18 as well as to an increase in the concentration of the embedded Al donor impurity. The optical transmittance and ellipsometry studies showed that the optical band gap is within 3.35…3.42 eV. All grown ZnO:Al thin films exhibit the wide NBE band within the ultraviolet range and the defect-related bands within the visible range. The PL of ZnO:Al films is dominated by a red-orange band at 2.08 eV, a yellow band at 2.25 eV, and a green emissions band at 2.55 eV, usually associated with the structural defects, namely, oxygen interstitials and oxygen and zinc vacancy as well as surface states. With increasing the substrate bias voltage the redistribution of the intensity of the red-orange emission band and yellow band is observed, which can be caused by the variation in surface states.

It was found that the negative bias voltage applied to the substrate holder during film growth allows us to increase the conductivity of ZnO:Al films by four times compared to ZnO:Al films deposited without an external bias voltage. This effect is due to more effective Al^{3+} donor impurity embedding into the ZnO lattice caused by the negative bias voltage applied to the substrate. The lowest value of the specific resistivity 4 mOhm·cm was achieved at negative substrate bias voltage V_{sb} = –30 V.

In summary, the application of substrate bias voltage as an additional parameter in magnetron sputtering allows effective influence on the structural, optical, and electrical properties of Al-doped ZnO films.

Acknowledgments

This work was supported by the research project of NAS of Ukraine “Optical, magnetic and thermoelectric properties of the new nanocomposites based on oxide materials”.

The authors are sincerely grateful to all defenders of Ukraine and emergency workers who made it possible to perform these studies and publish our results.

References

1. Zhou R., Wu X.-Y., Zhao Q. *et al.* One-step synthesis of multi-colored ZnO nanoparticles for white light-emitting diodes. *J. Lumin.* 2022. **252**. P. 119425. https://doi.org/10.1016/j.jlumin.2022.119425.

2. Liu W., Shi B., Xin Z. *et al.* High performance surface plasmon enhanced ZnO-Pt @ AlN core shell UV photodetector synthesized by magnetron sputtering. *Materials & Design.* 2024. **237**. P. 112542. https://doi.org/10.1016/j.matdes.2023.112542.
3. Baibara O., Radchenko M., Karpyna V., Ievtushenko A. A review of the some aspects for the development of ZnO based photocatalysts for a variety of applications. *Phys. Chem. Solid State.* 2021. **22**. P. 585. https://doi.org/10.15330/pcss.22.3.585-594.
4. Sun Y., Zhang W., Li Q. *et al.* Preparations and applications of zinc oxide based photocatalytic materials. *Advanced Sensor and Energy Materials.* 2023. **2**. P. 100069. https://doi.org/10.1016/j.asems.2023.100069.
5. Zhang L., Kang Y., Tang Y., Yu F. UV-activated ZnO–NiO heterojunction sensor for ethanol gas detection at low working temperature. *Mater. Sci. Semicon. Proc*. 2024. **169**. P. 107925. https://doi.org/10.1016/j.mssp.2023.107925.
6. Myroniuk D.V., Ievtushenko A.I., Lashkarev G.V. *et al.* Effect of electron irradiation on transparent conductive films ZnO:Al deposited at different power sputtering. *SPQEO*. 2015. **18**. P. 286–291. https://doi.org/10.15407/spqeo18.03.286.
7. Ellmer K., Welzel T. Reactive magnetron sputtering of transparent conductive oxide thin films: Role of energetic particle (ion) bombardment. *J. Mater. Res.* 2012. **27**. P. 765. https://doi.org/10.1557/jmr.2011.428.
8. Kiliszkiewicz M., Domaradzki J., Posadowski W. *et al.* Effect of sputtering power and oxygen partial pressure on structural and opto-electronic properties of Al-doped ZnO transparent conducting oxides. *Appl. Surf. Sci*. **670**. 2024. P. 160601. https://doi.org/10.1016/j.apsusc.2024.160601.
9. Gonçalves R.S., Barrozo P., Cunha F. Optical and structural properties of ZnO thin films grown by magnetron sputtering: Effect of the radio frequency power. *Thin Solid Films.* 2016. **616**. P. 265. https://doi.org/10.1016/j.tsf.2016.08.040.
10. Puthiyottil H., Thankamani P.R., Saji K.J. Exploring the effects of substrate and substrate temperature on the properties of radio frequency magnetron sputtered ZnO thin films. *Mater. Today Commun*. 2023. **36**. P. 106455. https://doi.org/10.1016/j.mtcomm.2023.106455.
11. Zhao Y., Hou S., Fang L.G. *et al.* The effect of negative substrate bias on the strain prosperities of ZnO Films deposited by PFCVAD. *Adv. Mater. Res.* 2011. **287-290**. P. 2373. https://doi.org/10.4028/www.scientific.net/amr.287-290.2373.
12. Brett M.J., Parsons R.R. Stoichiometry control mechanisms for bias-sputtered zinc-oxide thin films. *Canadian Journal of Physics.* 1985. **63**, No 6. P. 819. https://doi.org/10.1139/p85-132.
13. Chao L.-C., Lin S.-J., Chang W.-C. Growth, characterization and effect of substrate bias on ZnO prepared by reactive capillaritron ion beam sputtering deposition. *Nucl. Instrum. Methods Phys. Res. B.* 2010. **268**. P. 1581. https://doi.org/10.1016/j.nimb.2010.03.012.
14. Kwak D.-J. Effect of substrate bias voltage on the electrical properties of ZnO:Al transparent conducting film deposited on organic substrate. *Journal of the Korean Institute of Illuminating and Electrical Installation Engineers.* 2009. **23**. P. 78. https://doi.org/10.5207/JIEIE.2009.23.1.078.
15. Ievtushenko A.I., Karpyna V.A., Lazorenko V.I. *et al.* High quality ZnO films deposited by radio-frequency magnetron sputtering using layer by layer growth method. *Thin Solid Films*. 2010. **518**. P. 4529. https://doi.org/10.1016/j.tsf.2009.12.023.
16. Karpyna V., Ievtushenko A., Kolomys O. *et al.* Raman and photoluminescence study of Al,N-codoped ZnO films deposited at oxygen-rich conditions by magnetron sputtering. *phys. status solidi (b)*. 2020. **257**. P. 1900788. https://doi.org/10.1002/pssb.201900788.
17. Golovynskyi S., Ievtushenko A., Mamykin S. *et al.* High transparent and conductive undoped ZnO thin films deposited by reactive ion-beam sputtering. *Vacuum.* 2018. **153**. P. 204. https://doi.org/10.1016/j.vacuum.2018.04.019.
18. Yu P.Y., Cardona M. *Fundamentals of Semiconductors, Physics and Materials Properties.* Springer, Berlin, 1996.
19. Pramanik S., Mukherjee S., Dey S. *et al.* Cooperative effects of zinc interstitials and oxygen vacancies on violet-blue photoluminescence of ZnO nanoparticles: UV radiation induced enhanced latent fingerprint detection. *J. Lumin*. 2022. **251**. P. 119156. https://doi.org/10.1016/j.jlumin.2022.119156.
20. Zhao A., Luo T., Chem L. *et al.* Synthesis of ordered ZnO nanorods film on zinc-coated Si substrate and their photoluminescence property. *Mat. Chem. Phys.* 2006. **99**. P. 50. https://doi.org/10.1016/j.matchemphys.2005.10.013.
21. Kaschner A., Haboeck U., Strassburg M. *et al.* Nitrogen-related local vibrational modes in ZnO:N. *Appl. Phys. Lett.* 2002. **80**. P. 1909–1911. https://doi.org/10.1063/1.1461903.
22. Ievtushenko A., Tkach V., Strelchuk V. *et al.* Solar explosive evaporation growth of ZnO nanostructures. *Appl. Sci.* 2017. **7**, No 4. P. 383. https://doi.org/10.3390/app7040383.
23. Bundesmann C., Ashkenov N., Schubert M. *et al.* Raman scattering in ZnO thin films doped with Fe, Sb, Al, Ga, and Li. *Appl. Phys. Lett*. 2003. **83**. P. 1974–1976. https://doi.org/10.1063/1.1609251.
24. Artús L., Cuscó R., Alarcón-Lladó E. Isotopic study of the nitrogen-related modes in N^+-implanted ZnO. *Appl. Phys. Lett.* 2007. **90**. P. 181911. https://doi.org/10.1063/1.2734474.
25. Souissi H., Jabri S., Souissi A. *et al.* Activation of B1 silent Raman modes and its potential origin as source for phonon assisted replicas in photo-

luminescence response in N-doped ZnO nanowires. *J. Appl. Phys*. 2018. **123**. P. 025705. https://doi.org/10.1063/1.5011142.
26. Kaur G., Mitra A., Yadav K.L. Pulsed laser deposited Al-doped ZnO thin films for optical applications. *Prog. Nat. Sci.: Mater. Int.* 2015. **25**. P.12. https://doi.org/10.1016/j.pnsc.2015.01.012.
27. Oba F., Choi M., Togo A., Tanaka I. Point defects in ZnO: an approach from first principles. *Sci. Technol. Adv. Mater*. 2011. **12**. P. 034302. https://doi.org/10.1088/1468-6996/12/3/034302.

Authors and CV

Arsenii I. Ievtushenko, PhD, Head of Department of Physics and Technology of Photoelectronic and Magnetoactive Materials at the I. Frantsevych Institute for Problems of Materials Science, NAS of Ukraine. Author of more than 230 publications. His research interests include solid-state physics, functional materials, physical and chemical properties of oxide semiconductors.
https://orcid.org/0000-0002-8965-6772

Vitalii A. Karpyna, PhD, Senior Researcher at the Department of Physics and Technology of Photoelectronic and Magnetoactive Materials, I. Frantsevych Institute for Problems of Materials Science, NAS of Ukraine. Author of 154 publications. The main research activity covers the growth of thin films and nanostructures, investigation of these structure, optical and electrical properties of oxide semiconductors. E-mail: v.karpyna@ipms.kyiv.ua,
https://orcid.org/0000-0002-1834-3672

Sergii V. Mamykin, PhD, Head of Department of Kinetic Phenomena and Polaritonics at the V. Lashkaryov Institute of Semiconductor Physics, NAS of Ukraine. Author of over 90 publications and 5 patents. The area of his scientific interests includes plasmonics, sensorics and physics of photodetectors. E-mail: mamykin@isp.kiev.ua
http://orcid.org/0000-0002-9427-324X

Olexander I. Bykov, PhD in Engineering. Leading Researcher at the I. Frantsevych Institute for Problems of Materials Science, NAS of Ukraine. Author of more than 200 scientific publications. His research interests include solid state physics, XRD.
https://orcid.org/0000-0001-6959-3498

Petro M. Lytvyn, PhD, Head of Department at the V. Lashkaryov Institute of Semiconductor Physics, NAS of Ukraine. His research focuses on solid-state physics, functional materials, and nanophysics of semiconductors and related materials. He has authored over 350 peer-reviewed publications, holds 10 patents, and has contributed to nine monographs, advancing knowledge in these fields. E-mail: plyt@isp.kiev.ua,
https://orcid.org/0000-0002-0131-9860

Oleksandr F. Kolomys, PhD, Senior Researcher at the Laboratory of submicron optical spectroscopy, V. Lashkaryov Institute of Semiconductor Physics, NASU. Authored over 130 publications, 3 patents, 3 chapters in textbooks. The area of his scientific interests includes Raman and luminescent microanalysis of light emitting properties, structure, composition, electronic and phonon excitations in solids. E-mail: olkolomys@gmail.com,
https://orcid.org/0000-0002-1902-4075

Andrii A. Korchovyi, PhD, Senior Researcher at the Laboratory for scanning probe microscopy, V. Lashkaryov Institute of Semiconductor Physics, NASU. Authored over 100 publications. The area of his scientific interests includes atomic force microscopy, physical and chemical properties of semiconductor materials and nanostructures for modern micro- and nano-electronics.
E-mail: akorchovyi@gmail.com,
https://orcid.org/ 0000-0002-8848-7049

Sergii P. Starik, PhD, Senior Researcher, Head of Laboratory “Nanostructural and crystallo-physical researches” at the V. Bakul Institute for Superhard Materials, NASU. Authored over 100 publications, 7 patents. His research interests include diagnostic of physics properties of materials. E-mail: starik@ism.kiev.ua,
https://orcid.org/0000-0003-1991-3275

Viktor V. Bilorusets, Junior researcher of the Laboratory “Nanostructural and crystallo-physical researches” at the V. Bakul Institute for Superhard Materials, NASU. The area of scientific interests includes the vacuum manufacture coatings and diagnostic of physics properties for materials.

Vadym I. Popenko, PhD, Researcher at the V. Lashkaryov Institute of Semiconductor Physics. Field of research: optical, structural and electrical properties of carbon nanostructures and their composites with metals, their study using Raman, photoluminescence and ellipsometry spectroscopy and XRD methods; mechanisms of interaction of microwave radiation with carbon-containing polymer nanocomposites. E-mail: kurosavakata@gmail.com, https://orcid.org/0009-0005-3116-9380

Volodymyr A. Baturin, PhD, Member of Academic Council, Principal research assistant, Deputy head of the Department, Head of Laboratory at the Institute of Applied Physics, NASU. The area of scientific interests includes the manufacture of nanostructured materials, physics of nuclei, elementary particles and high energies. https://orcid.org/0000-0001-6171-8575

Viktor V. Strelchuk, Doctor of Sciences, Professor, Leading Researcher at the Laboratory of submicron optical spectroscopy, V. Lashkaryov Institute of Semiconductor Physics. Authored over 300 publications, 10 patents, 6 textbooks. Field of research: physics of semiconductors, Raman and photoluminescence spectroscopy of semiconductors, nanostructures and nanoscale materials. E-mail: viktor.strelchuk@ccu-semicond.net, https://orcid.org/0000-0002-6894-1742

Oleksandr Yu. Karpenko, Junior Researcher at the Institute of Applied Physics, NASU. Author of more than 40 publications, 2 patents. Research interests include the influence of surface modification on the probability of high-vacuum break-down, the technology of thin films, and ion implantation. https://orcid.org/0000-0001-9280-082X

Authors' contributions

Ievtushenko A.I.: key ideas, conceptualization, investigation, writing – original draft, supervision.
Karpyna V.A.: performed experiments of transmittance, analyzing the data.
Kolomys O.F.: analyzing the data of RTIR, writing and editing FTIR part.
Mamykin S.V.: conceptualization, writing – review and editing.
Bykov O.I.: performed XRD measurements.
Lytvyn P.M.: methodology, data curation, writing – review & editing, visualization.
Korchovyi A.A.: investigation, formal analysis.
Starik S.P.: performed SEM and EDX measurements.
Bilorusets V.V.: sample preparation, investigation.
Popenko V.I.: investigation, formal analysis.
Strelchuk V.V.: validation of FTIR experimental data.
Baturin V.A.: sample preparation, thin films ion implantation.
Karpenko O.Yu.: sample preparation, manufacture of ZnO films.

Вплив напруги зміщення підкладки на властивості легованих Al плівок ZnO, вирощених магнетронним напиленням

А.І. Євтушенко, В.А. Карпина, О.Ф. Коломис, С.В. Мамикін, П.М. Литвин, О.І. Биков, А.А. Корчовий, С.П. Старик, В.В. Білорусець, В.І. Попенко, В.В. Стрельчук, В.А. Батурин, О.Ю. Карпенко

Анотація. Метою нашої роботи є дослідження впливу напруги зміщення, прикладеної до Si (100) та скляних підкладок, на структуру, оптичні та електричні властивості тонких плівок ZnO:Al, осаджених на них методом радіочастотного магнетронного розпилення. Ми застосували метод пошарового вирощування при магнетронному розпиленні. Для характеристики зразків використовували рентгенівську дифракцію, атомно-силову мікроскопію, комбінаційне розсіювання світла, фотолюмінесценцію, інфрачервону спектрометрію з перетворенням Фур'є, багатокутову еліпсометрію, оптичне пропускання та електричні вимірювання. Виявлено, що від'ємна напруга зсуву, прикладена до тримача підкладки під час вирощування плівки, дозволяє збільшити провідність плівок ZnO:Al у чотири рази порівняно з плівками ZnO:Al, осадженими без прикладання напруги зміщення. Концентрація донорної домішки Al у плівках ZnO:Al зростає зі збільшенням від'ємної напруги зміщення, прикладеної до підкладки.

Ключові слова: плівки ZnO:Al, магнетронне розпилення, напруга зміщення підкладки, рентгеноструктурний аналіз, коефіцієнт пропускання, електропровідність.